Journal of The Electrochemical Society, **166** (8) D244-D251 (2019)
0013-4651/2019/166(8)/D244/8/$38.00 © The Electrochemical Society

Ultrasound Assisted Electrodeposition of Cu-SiO_2 Composite Coatings: Effect of Particle Surface Chemistry

L. N. Bengoa,[1,z] A. Ispas,[2,*] J. F. Bengoa,[3] A. Bund,[2,*] and W. A. Egli[1]

[1] *Centro de Investigación y Desarrollo en Tecnología de Pinturas-CIDEPINT (CICPBA-CONICET-UNLP), B1900AYB La Plata, Argentina*
[2] *Electrochemistry and Electroplating Group, Technische Universität Ilmenau, 98693 Ilmenau, Germany*
[3] *Centro de Investigación y Desarrollo en Ciencias Aplicadas-CINDECA, (CICPBA-CONICET-UNLP), 1900 La Plata, Buenos Aires, Argentina*

Electrodeposition of Cu-SiO_2 composite coatings from an alkaline non-cyanide electrolyte containing glutamate as complexing agent was studied. Silica mesoporous particles were synthesized using a modified Stöber methodology, and later their surface chemistry was changed by functionalizing them with 3-aminopropyltriethoxysilane. Particles microstructure and morphology were characterized (SEM, TEM, XRD) and their charging behavior in several electrolytes was studied through ζ-potential measurements. Galvanostatic deposition was performed in electrolytes containing both as-prepared and functionalized SiO_2 at various current densities, and the influence of ultrasonic irradiation (37 Hz) was evaluated. For some experiments, 1.5 g L^{-} of Polyquaternium 7 were added to the solution. SEM and XRD were used to characterized coatings morphology and microstructure, whereas EDS was used to estimate SiO_2 wt%. The results showed that the effect of ultrasound on the codeposition process depends on current density and particle surface chemistry. All the trends observed in this study could be explained taking into account ζ-potential values recorded and previously reported theories. Adjusting the experimental conditions, it was possible to obtain deposits with SiO_2 contents of ≈5 wt%. Finally, it was found that both ultrasonic irradiation and Polyquaternium 7 affect the morphology and crystal orientation of the deposits.
 [DOI: 10.1149/2.0181908jes]

Manuscript submitted February 12, 2019; revised manuscript received April 8, 2019. Published April 23, 2019.

Composite functional coatings have been gaining relevance in the last decades due to the fast development of novel technologies which require high performance materials. Among these, metal-based composites present several attractive characteristics since they combine the mechanical and physical properties of metals (ductility, high thermal and electrical conductivity) with those of the dispersed phase. The latter has traditionally consisted in ceramic materials that improve the mechanical properties, such as hardness,[1] wear resistance[2–5] and lubrication[6–8] of the base metal, though some polymeric[9] and even metallic[10] particles have also been incorporated. In recent years these types of composites have proved to be suitable materials for electrocatalysis,[11] energy storage and electronics.[12] Hence, these findings indicate that metal-based composites possess a high potential but many of their applications are still to be discovered.

Composite metallic coatings can be produced using several different techniques, which include electrodeposition, powder metallurgy, thermal spraying and vacuum deposition.[12] Despite being one of the oldest methods to obtain this kind of deposits, electrochemical deposition still stands out among the others due to the simple equipment required and its low operation costs (no high vacuum or temperatures needed). On the other hand, this technology involves the use of electrolytes which usually contain hazardous substances, both to the environment and human health, leading to high treatment and disposal costs.[13,14] This is one of the major drawbacks of electroplating, and has been the focus of many academic investigations and industrial developments in recent years.[15–21] In particular, lots of efforts have been put in finding a replacement for alkaline cyanide-based electrolytes still being used in copper plating industry in some countries.[22–24] As a result, many environmentally friendly electrolytes have been proposed as alternatives to traditional plating baths but the suitability of these formulations to obtain composite deposits has not been thoroughly evaluated. Since particle incorporation strongly depends on the chemistry of the solution, this kind of studies should be performed to scale-up the production of functional composite coatings from eco-friendly electrolytes in the future.

The first report on the preparation of a composite coating through electrodeposition in 1928,[25] triggered a large number of investigations devoted either to the development of these materials or the understanding of the underlying phenomena. Several metal-particle systems have been considered so far,[6,7,26–44] of which Cu-based composites are the ones that have attracted the most interest.[33,45–50] The latter is due to copper's good corrosion resistance, appearance and high thermal and electrical conductivity, and the possibility to improve its mechanical properties by the incorporation of particles in the deposit. For instance, dispersion of a second phase, regardless of its composition, in the metallic matrix will cause an increase in the deposit hardness through a dispersion strengthening effect.[1,51] Moreover, if particles like graphite, CNT or PTFE are incorporated, self-lubricating Cu deposits with a good tribological behavior can be obtained, which could be used as a protective coating in car engines.[25] Some authors have even used this methodology to develop copper composites coatings with specific properties to be used as electrical contacts[47] and heat sinks in integrated circuits.[52] Therefore, it is evident that electrochemical codeposition is a versatile technique that allows the production of novel coatings with special properties.

However, for some metal-particle systems only low incorporation rates have been achieved.[53] The reasons behind this issue are not entirely clear, probably because the underlying mechanism through which particles are embedded in the metallic matrix has not been yet completely unveiled despite the several attempts that have been made to explain this process.[44,54–56] Nevertheless, the results gathered throughout the years have showed that the incorporation rate depends on several factors related to particles nature, bath chemistry and deposition conditions,[57,58] and thus, many alternatives have been proposed to increase particle content in the deposit. Among these, the use of ultrasound (US) during electrodeposition constitutes a promising approach, which has already proved to be beneficial for the deposition of various composite coatings.[5,53,59,60] Furthermore, cavitation phenomena that take place in the electrolyte when an ultrasonic field is applied may improve particle dispersion, as well as the electrochemical process itself (mass and/or charge transfer phenomena, current efficiency) and the final coating's characteristics (crystal orientation, grain size, surface morphology).[61]

On the other hand, recent findings indicate that the adsorption of electroactive species onto particle surface promotes their incorporation into the growing deposit,[62] in agreement with the main postulate of Celis et al. model.[55] This means that high particle content can be attained adjusting the chemistry of the electrolyte (e.g. additives, pH) to maximize cation uptake. However, the latter is not always possible since it might affect the electrodeposition process which, in turn, could prevent the obtention of good quality coatings. A different approach, proposed by Terzieva et al.,[45] consists in modifying the particle

*Electrochemical Society Member.
[z]E-mail: l.bengoa@cidepint.ing.unlp.edu.ar

surface chemistry instead of changing the bath composition. For their study, the authors used mesoporous silica particles, which can be easily functionalized through chemical reaction with siloxanes.[63–65] The latter allows grafting of specific functional groups such as -NH_2 or -SH, with different electronegativity to enhance ion adsorption in a large variety of electrolytes. It is worth mentioning that despite the potential of this methodology to achieve higher incorporation rates, it has not been widely studied.

Based on what has been described in previous paragraphs, the present work deals with the deposition of composite coatings from a novel glutamate-based alkaline electrolyte (Cu**Glu**).[66] This electrolyte has been recently proposed as an alternative to cyanide-based copper plating baths, and particle codeposition in this medium has not been investigated thoroughly. The goals of this investigation are both to achieve high particle content Cu-based composites and, at the same time, confirm the importance of the adsorption step in the electrocodeposition, process providing further insight into this phenomenon. To that end, mesoporous silica particles were synthesized and later amino-functionalized to improve Cu^{2+} adsorption. Moreover, the use of low-frequency ultrasound agitation to improve the incorporation rate was investigated, an approach which has been scarcely used but has shown a great potential. Finally, the influence of Polyquaternium 7 (P-7), a common brightener used in Cu**Glu** electrolytes**,** on the incorporation rate and the deposits properties was evaluated. Particle content, morphology and crystal orientation of the resulting deposits were investigated, to determine the best operation conditions to obtain good quality deposits with high silica content.

Experimental

Particle synthesis and characterization.—Silica particles were prepared using a variation of the Stöber synthesis proposed by Grün et al.,[67] which mainly consists in the hydrolyzation and condensation of tetraethyl orthosilicate (TEOS, 99%, Aldrich). The reacting solution was prepared mixing 50 mL of distilled water, 30 mL NH_4OH (Cicarelli, 28% p/p), 2.5 g of n-hexadecyltrimethylamonnium bromide (CTMABr,98%, Sigma), 75 mL of absolute ethanol (Cicarelli, 99.5%) and 5 mL of TEOS at room temperature to achieve a molar composition of 1 TEOS:0.3 CTMABr:11 NH_4OH:58 ethanol:144 H_2O. The resulting gel was kept under stirring at 30°C for 2 h, and then the obtained solid product was separated by filtration, washed with water and ethanol several times and dried at room temperature. Finally, the sample was calcined up to 550°C in air atmosphere for 3 h, with a heating rate of 5°C min^- to remove the CTMABr from the pores. This method yields a monodispersed distribution of spherical SiO_2 particles with a hexagonal arrangement of pores with diameters between 15–100 Å, known as MCM-41[68] (M41). This name will be used throughout this work to refer to the as-prepared particles. A fraction of these particles was functionalized by mixing 1 g of M41 with 1 mL of 3-aminopropyltriethoxysilane (APTES, 98%, Sigma) in toluene (100 mL) under vigorous stirring at 80°C for 6 h. The solid was later filtered and washed with ethanol and water several times to eliminate any non-reacted physisorbed APTES. This sample was named MNH_2.

Specific surface area (S_g), specific pore volume (V_p) and pore diameter (D_p) of both samples were determined by N_2 adsorption-desorption measurements at −196°C (Micromeritics ASAP 2020 V1.02 E). The pore size distribution was estimated using the Barret-Joyner-Halenda method (BJH). X-ray diffraction (XRD) patterns were recorded to confirm the pore microstructure of M41 materials. Furthermore, scanning electron (SEM) and transmission electron microcopy (TEM) were performed to determine particle morphology and size.

Zeta-potential (ζ) measurements were carried out using a Malvern Zetasizer Nano ZS (ZEN3600) to characterize charging behavior of particles in different electrolytes. To that end, 10^{-3} M KNO_3 and 10^{-3} M Na_2SO_4 were prepared to estimate the iso-electric point (IEP) and to identify possible interactions between surface groups and SO_4^{2-} anions, respectively. In addition to this, ζ-potential was measured in a diluted Cu**Glu** electrolyte with a 0.01 M Cu^{2+} ($CuSO_4$, 99%) and 0.2 M sodium glutamate (Glu,$^{2-}$ abcr 99%), both in the absence and the presence of 0.15 g L^{-1} Polyquaternium-7 (P-7), a positively charged polymer used as additive later in deposition experiments. The dilution proposed for these experiments is necessary due to the high ionic strength of the plating solution (see following paragraph) which would otherwise hinder the determination of ζ-potential values.[29] Cu^{2+} and $\mathbf{Glu}^{2-}$ concentrations were chosen based on equilibria calculation made with MEDUSA software,[69] in order to have the same speciation in both the diluted and the plating electrolyte. For all these experiments, a particle concentration of 0.5 g L^- was used whereas the pH range considered was 2–10. The latter was adjusted with KOH and HNO_3 for measurements in 10^{-3} M KNO_3 solutions while NaOH and H_2SO_4 were used for both Na_2SO_4 and Cu**Glu** electrolytes.

Deposition experiments and deposits characterization.—The plating solution used in this study was a 0.2 M Cu^{2+} and 0.6 M $\mathbf{Glu}^{2-}$ electrolyte with a pH of 8,[66] adjusted by addition of KOH. To this solution, 1.5 g $L^-$of P-7 were added in some tests to evaluate its influence on the codeposition of silica and copper. Electrodeposition experiments were conducted using a three-electrode configuration together with a Biologic SP-150 galvanostat/potentiostat. Low-carbon steel disks with a 0.25 dm diameter were used as substrates, which were placed in a dismountable RDE leaving an active area of 0.025 dm^2. A pure copper disk (0.196 dm^2) anode was located at the bottom of the cell facing the RDE, whereas a saturated Ag|AgCl (0.197 V vs NHE) electrode served as reference electrode. Steel substrates were degreased with acetone, rinsed with distilled water and pickled in a H_2SO_4 1:10 v/v solution at 40°C for 60 s just before deposition. Cu-MCM deposits were obtained at current densities (j) in the 1−5 A dm^{-2}range and plating time was adjusted to reach a 5 μm thickness considering a 100% faradaic efficiency.[66] Throughout this study, plating was performed at a temperature of 60°C and with a particle concentration of 5 g L^-.

Experiments were carried out in a 250 mL beaker which was placed in the center of an ElmasonicP 120 H ultrasonic bath (nominal power 300 W) with a built-in thermostat, at a controlled depth. To ensure reproducibility, the volume of plating solution in the beaker (150 mL) as well as the water level in the bath, were kept constant. Ultrasonic irradiation with a 37 Hz frequency was applied at nominal powers of 70% and 100%. The latter correspond to power densities of 1.62 and 2.20 W cm^{-3} estimated using the calorimetric method.[53,59] Deposition was also performed in the absence of US irradiation (silent) rotating the RDE at 200 rpm to prevent particles from settling. To properly assess the effect of US on particle incorporation, the working electrode was rotated at the same speed even in the presence of US irradiation. Each day, particles were dispersed for 30 min using US (nominal power 100%) prior to any deposition experiment. Moreover, when two experiments in silent conditions were performed consequently, 5 min US agitation was applied to avoid particle agglomeration.

The surface morphology and the cross-section of the deposits was examined by scanning electron microscopy (SEM) using a Hitachi S4800 microscope. The content of SiO_2 was estimated using energy dispersive spectroscopy (EDS) performed on the surface of the deposits. XRD patterns were recorded with an X-ray diffractometer Bruker AXS D 5000 operating with Cu-Kα radiation. The detector was swept between 10 and 90 ° with a 0.04 ° step and 2 seconds per step. The preferred crystal orientation of the Cu deposits was assessed by means of the relative texture coefficient (RTC), calculated using Eq. 1.[29,59,70]

$$RTC_{hkl} = \frac{I_{hkl}/I^0{}_{hkl}}{\sum_1^3 I_{hkl}/I^0{}_{hkl}} \times 100 \quad [1]$$

where I_{hkl} and $I^0{}_{hkl}$ are the diffraction intensities of the crystal plane (hkl) in the sample and a standard Cu powder sample with random orientation, respectively. The sum in the denominator only considers the planes (111), (200) and (220) which are the most important

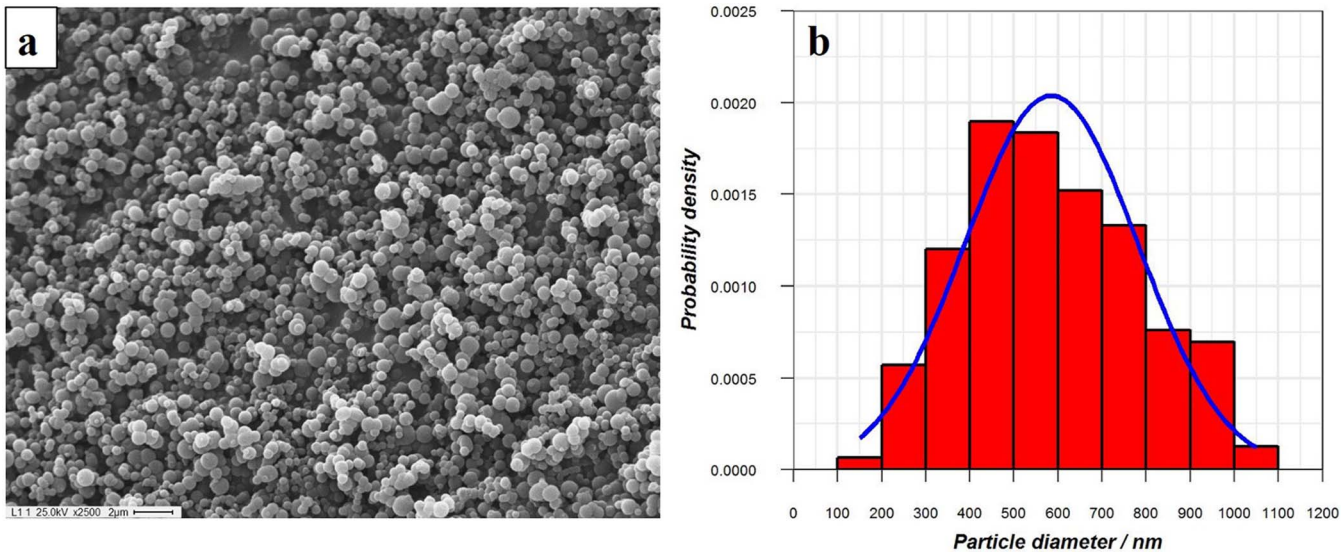

Figure 1. (a) SEM image (2500 X) and (b) particle size distribution of M41 particles. The experimental data was fitted to a Gaussian distribution for comparison purposes (blue line).

ones for Cu (higher intensities) and are relevant for texture analysis.[66] Therefore, planes with RTC values above 33% (100/3%) are considered to be preferred crystal orientations.[29]

Results and Discussion

The synthesized particles are spherical in shape and present a monodisperse particle size distribution with an average diameter of 584 nm (Figs. 1a and 1b). The XRD patterns recorded at low 2θ values (1.5 – 9°) showed a main peak around 2.4° and two small broad peaks in the 4 – 5° range, which can be ascribed to the characteristic 2D hexagonal arrangement of mesopores of M41 microstructure (Fig. 2).[71] Fig. 3 shows a HRTEM image of these particles, in which pores with diameters around 3 nm can be clearly observed. These results confirm that the synthesis process was successful, yielding the desired material. Functionalization had no effect on M41 microstructure in agreement with previous studies[72] (not shown).

The N_2 adsorption results for both types of particles (Table I) show that functionalization causes a reduction in the specific surface area, pore volume and pore diameter. This effect has been previously observed[73] and is an indication of the successful attachment of amino propyl functions to the surface of SiO_2 particles. The presence of

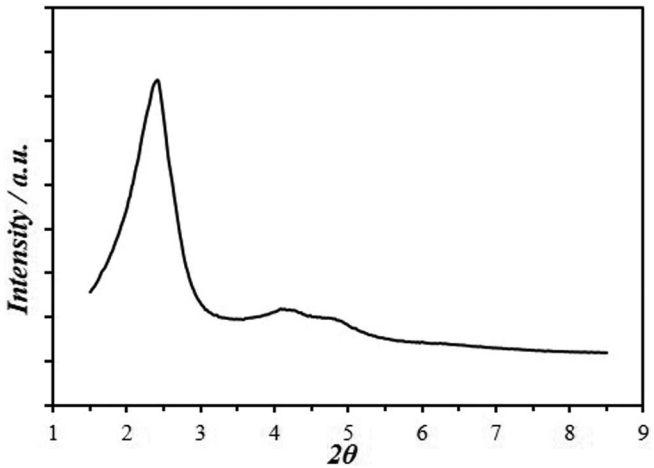

Figure 2. Low angle XRD pattern of M41 particles.

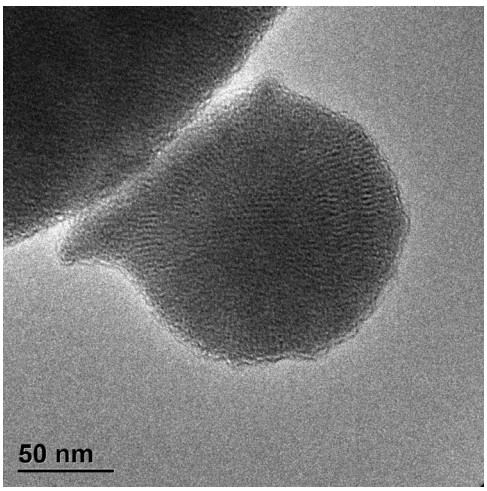

Figure 3. HRTEM of M41 sample.

these large molecules inside the pores reduces the available space for N_2 adsorption, leading to a decrease in the aforementioned parameters. Moreover, these organic groups modify the adsorption enthalpy between N_2 and the silica surface, evidenced by a change in the C_{BET} constant from 95.8 to 39.3.[72]

Once the particle's microstructure was determined and the functionalization confirmed, their surface chemical behavior was characterized by ζ-potential measurements and Cu^{2+} adsorption experiments. The surface charge and the adsorption of the electroactive species have been proposed as relevant parameters/steps for the

Table I. Textural properties of SiO_2 particles before and after functionalization determined by N_2 adsorption.

Sample	$S_g/m^2\ g^{-1}$ [a]	$V_p/m^3\ g^{-1}$ [a]	D_p/nm [b]	C_{BET}
M41	971.4	0.7	2.4	95.8
MNH_2	768.3	0.4	2.2	39.3

[a]BET method.
[b]BJH method.

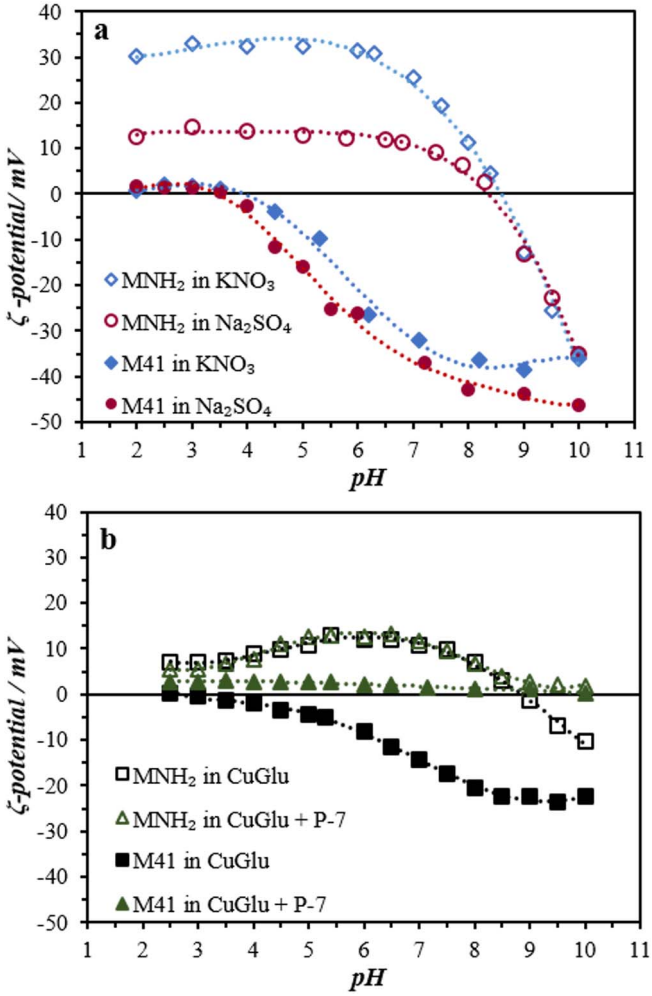

Figure 4. ζ-potential of M41 and MNH_2 particles as a function of pH in various electrolytes: (a) KNO_3, and Na_2SO_4; (b) diluted Cu**Glu** and diluted Cu**Glu** + P-7.

codeposition of particles by different authors,[54,55] and for that reason these determinations will provide important information for the analysis of the incorporation behavior of SiO_2 particles in Cu**Glu** electrolytes. Figs. 4a and 4b show the variation of ζ-potential of M41 and $MNH_2$with pH in different electrolytes. In a 10^{-3}M KNO_3 solution, M41 particles were positively charged for pH values below 3.7 due to protonation of free silanols (-Si-OH),[74] in agreement with reported values of the isoelectric point (IEP) for silica particles.[75–77] The functionalization process replaces some -OH groups with aminopropyl functionalities with a pK_a in the 9–10 range, which resulted in a shift of the IPE to higher pH values (≈8.6) (Fig. 4a). Similar trends were observed for both particles in a Na_2SO_4 solution, without a significant variation in the IEP. However, for MNH_2 the presence of SO_4^{2-} ions reduces the magnitude of ζ-potential for pH values in which the particles have a net positive charge (i.e. pH < IEP). The latter can be ascribed to the adsorption of sulfate ions on the positively charged surface through an electrostatic interaction, as has been previously reported for other materials.[29,75] It is worth noting that this ion (SO_4^{2-}) is present in high concentrations in the plating bath and its role in the charging behavior of particles must be known to understand their surface chemistry.

In a diluted Cu**Glu** electrolyte M41 particles showed a negative ζ-potential in the whole pH range studied. At pH < 3.7 (IEP measured in KNO_3) negative glutamate species ($H\mathbf{Glu}^-$)[78] may adsorb on the positively charged SiO_2 surface, changing the sign of the net charge on the particle's surface. As the pH of the solution was shifted from IEP to higher values, a decrease in ζ-potential was observed as was observed in KNO_3 or Na_2SO_4 electrolytes. This is probably the result of both silanol deprotonation and further glutamate uptake. Moreover, according to Vlasova[79] Cu^{2+} adsorption on SiO_2 occurs at pH above 5.5, which is likely to affect the magnitude of the ζ-potential but does not change the sign of the net surface charge.

Table II. Electrode potential registered (saturated Ag/AgCl) during galvanostatic experiments.

j/A dm^{-2}	E/V[a]	E_{PZC}/V[b]
−1	−0.53	−0.25
−2.5	−0.81	
−5	−1.15	

[a]Reported values are an average of the recorded potentials during deposition experiments at a given j.
[b]This value corresponds to the E_{PZC} of a Cu electrode in a Cu**Glu** electrolyte with pH = 8 and was taken from Reference 63.

In contrast, positive ζ-potentials were registered for MNH_2 in a diluted Cu**Glu** up to pH ≈8.8 (Fig. 4b), as was observed in KNO_3 and Na_2SO_4 electrolytes (Fig. 4b, IEP = 8.6).Between 2 < pH < 3.5 a virtually constant ζ-potential was observed, which was lower than the values measured for the same particles in other electrolytes (Fig. 4a). This can be attributed to the adsorption of both SO_4^{2-} and $H\mathbf{Glu}^-$ through an electrostatic interaction with NH_3^+ at the surface of functionalized silica. As pH was increased from 3.5 to 6.5, a rise in ζ-potential was observed which might be the result of copper-glutamate complexes formation at the surface of the particles through a reaction like the one depicted in Eq. 2. It has been proven that Cu^{2+} uptake on amino modified silica is already significant at pH = 5[64] and that glutamate can enhance copper adsorption on alumina through the formation of ternary surface complexes, even in acidic conditions.[80,81] Therefore, it is plausible that Cu^{2+} adsorption from a Cu**Glu** solution starts taking place at a pH ≈ 3.5. According to the proposed mechanism (Eq. 2) negative charges on the surface of MNH_2 (adsorbed anions) would be progressively replaced by neutral species as pH increases, leading to a small increase in the net surface charge. It should be mentioned that despite adsorption of either $\mathbf{Glu}^{2-}$ or complexes, the sign of the surface charge is still governed by NH_2 protonation (positive ζ-potential). A further increase in pH yielded a decrease in ζ-potential, which became negative for pH > 8.8 due to deprotonation of $NH_3^+$and SiOH that did not react during the functionalization procedure.

$$SiO - Si(CH_2)_3NH_3^+ + Cu^{2+} + \mathbf{Glu}^{2-} \rightarrow SiO - Si(CH_2)_3NH_2 - Cu\mathbf{Glu} + H^+ \quad [2]$$

Finally, measurements performed in the presence of P-7 showed that this additive adsorbs on both particles only for pH > IEP, conditions in which their surface has a net negative charge. Taking into account that P-7 has positive charges in its structure, an electrostatic interaction between this polymer and particles is likely to take place leading to a change in the sign of ζ-potential in this pH range.

Fig. 5 shows the incorporation rate of M41 and MNH_2 particles in the presence and in the absence of P-7 at different experimental conditions, where it can be clearly seen that functionalization improves particle incorporation. In general, particle content decreased as current density was raised, although deviations from this behavior were observed for functionalized SiO_2 in the presence of P-7 (Fig. 5b). The influence of j on the amount of SiO_2 registered is in agreement with previously reported results[29,42,82] and has been explained in detail somewhere else.[56,62] Briefly, as current density increases, the electrode potential (E) shifts away from the potential of zero charge (E_{PZC}) (Table II) favoring the interaction between the electrode and water molecules. This results in a strongly attached hydration layer which hinders particles from reaching the electrode surface, leading to lower incorporation rates.

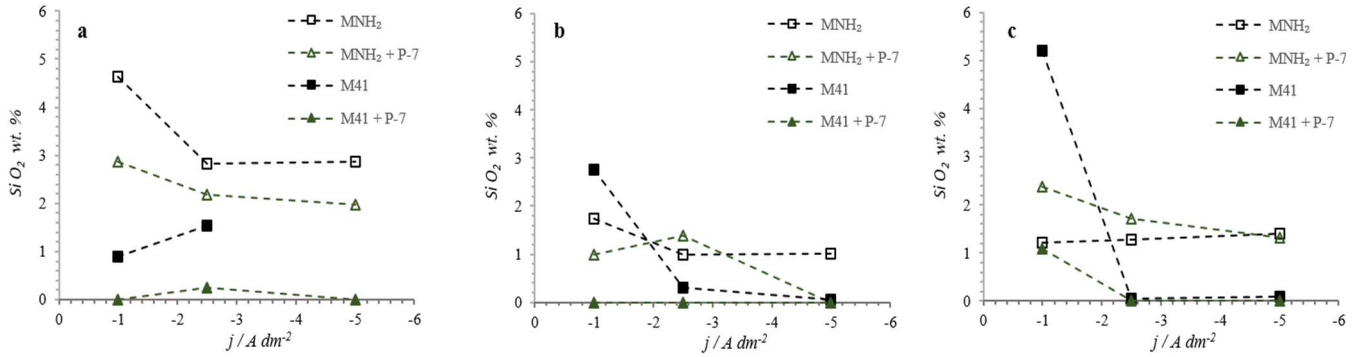

Figure 5. SiO_2 content (wt%) of Cu composite coatings obtained from a Cu**Glu** plating bath without and with 1.5 g L^{-} of P-7 under (a) silent conditions and applying (b) 1.62 W cm^{-3} and (c) 2.20 W cm^{-3} US irradiation. Results for both M41 and MNH_2 are shown.

For M41 sample, ultrasonic irradiation significantly promoted particle incorporation at $j = -1$ A dm^{-2} making it possible to obtain deposits with a content of SiO_2 five times larger than in silent conditions (Fig. 5c). However, this beneficial effect was not observed at higher current densities and the results even suggested that US may reduce the number of particles in the coating. A possible explanation for this behavior relies on the fact that even though US irradiation enhances particle flux toward the electrode, it would also tend to remove particles that are loosely adsorbed on the surface of the electrode. Hence, at low current densities, i.e. low $E\text{-}E_{PZC}$, it is likely that particle-electrode interactions are strong enough for the particle to remain at the electrode surface and eventually be embedded in the growing deposit. Addition of P-7 to the plating bath caused a considerable decrease in the amount of SiO_2 regardless of deposition conditions. Since P-7 adsorbs on M41 particles surface (see Fig. 4b), it blocks active sites which might have interacted with Cu^{2+} or Cu^{2+}-$\mathbf{Glu}^{2-}$ complexes otherwise. Thus, Cu^{2+} adsorption is hampered under these conditions, which leads to lower incorporation rates.[55,62]

When functionalized particles were added to the solution, a higher content of SiO_2 in the deposit was obtained for most experimental conditions, which suggests that the presence of amino groups at the particle surface enhances Cu^{2+} uptake. Nevertheless, for these particles US irradiation had a negative effect on the codeposition of Cu and SiO_2 both in the absence and presence of P-7. This behavior can be attributed to the agglomeration of MNH_2 particles in the electrolyte as a consequence of their low surface charge in this medium (Fig. 4b). Hence, particles have a larger effective size than not functionalized M41 (as shown in Fig. 6) and are more prone to be removed from the electrode surface by the shear forces induced by US. Moreover, bigger particles have a greater tendency to settle, moving away from the electrode and reducing the particle concentration at the surface. Finally, addition of P-7 to the solution had no clear effect on the incorporation rate, since a slight decrease in SiO_2 content was observed in silent conditions while a small increase was registered at 2.20 W m^{-3}. These results are consistent with ζ-potential measurements, which showed that this additive has a negligible effect on MNH_2 particles surface charge at pH = 8. Therefore, these variations could stem from P-7 adsorption as well as uncertainties in the SiO_2 wt% determination.

Regarding coating morphology, US irradiation promoted the formation of nodules on the surface of the deposit only at low j values and suppressed the formation of cracks (Fig. 7), a common feature of Cu deposits obtained from Cu**Glu** electrolytes.[66] However, if the content of silica in the deposit is high no nodules could be detected even at an ultrasonic power of 2.20 W m^{-3}. It is possible that particles act as additional nucleation sites avoiding the growth of large nodular structures. The aforementioned effects were not observed for higher current densities, in agreement with results obtained by Camargo et al.[53] Likewise, a cracks-free nodular morphology was observed after addition of P-7, in silent conditions for the whole j range considered in this work (Figs. 8). Under these conditions, application of US prevented nodule formation, yielding smooth surfaces. Finally, it is noteworthy that current density had no significant effect on coating morphology.

To evaluate the effects of the deposition parameters on microstructure and crystal orientation, the XRD patterns of the coatings were recorded for 2θ values between 10 – 90°. Figs. 9a, 9b and 9c show the changes in $RTC_{(hkl)}$ values induced by US irradiation and current density for samples obtained from electrolyte containing MNH_2. It can be seen that under silent conditions, deposition takes place preferentially following the <111> direction regardless of current density, leading to $RTC_{(111)}$ values of about 50%. Even though a rise in j slightly reduced $RTC_{(111)}$ and increased $RTC_{(200)}$, the preferred crystal orientation remained unchanged. Similar results were obtained for pure Cu deposits electrodeposited from a Cu**Glu** electrolyte.[66] The data in Fig. 9 also indicates that US irradiation promoted the development of a (220) texture at low j. This change in the preferred crystal orientation becomes more significant as US power is increased, reaching a

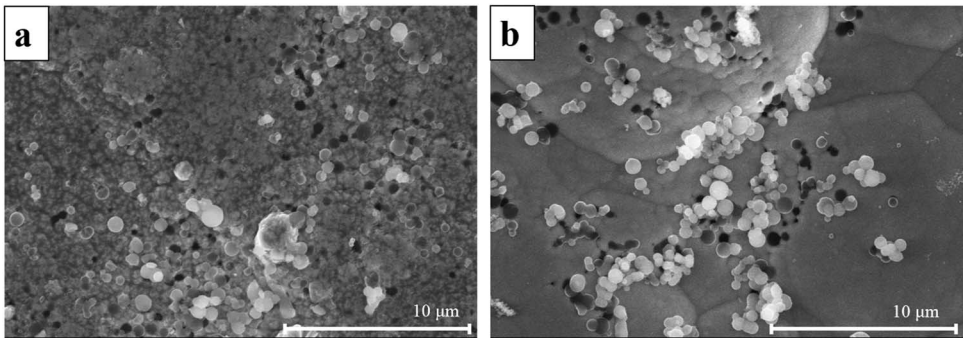

Figure 6. SEM images (5000 X) of Cu-SiO_2 composite coatings deposited at $j = -1$ A dm^{-2} and: (a) 2.20 W cm^{-3} US irradiation with M41; (b) silent conditions with MNH_2.

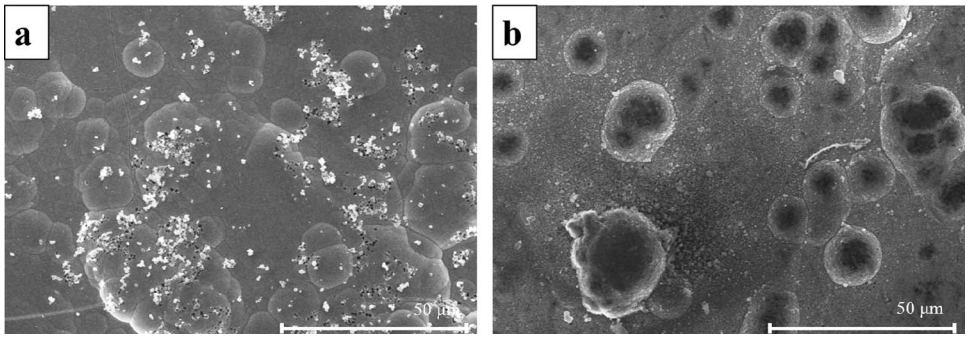

Figure 7. SEM images (1000 X) of deposits obtained $j = -1$ A dm^{-2} from a bath without P-7 containing MNH_2: (a) silent and (b) 2.20 W cm^{-3} US irradiation.

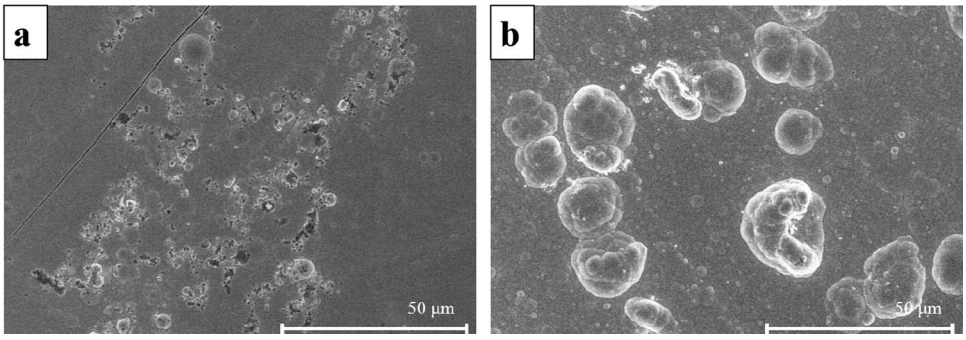

Figure 8. Morphology of Cu-M41 coatings deposited at $j = -2.5$ A dm^{-2} and silent conditions (a) in the absence and (b) the presence 1.5 g L^{-} of P-7 (1000 X).

$RTC_{(220)}$ of 92.6% at 2.20 W cm^{-3}. However, at higher current densities no considerable influence of US in coatings texture was detected, which is consistent with results previously reported by Camargo et al.[29] This behavior could be attributed to modifications in the crystallization mechanism caused by the presence of ultrasonic waves in the electrolyte. The latter would provide additional energy which might allow adatoms to relocate in the growing surface. Nevertheless, this could only happen if the number of adatoms is rather small at a certain time so there is available space on the surface for them to move freely. At high deposition rates, adatoms are generated at a higher pace and thus relocation may be hampered, which in turn would limit the effect of US in crystal orientation.

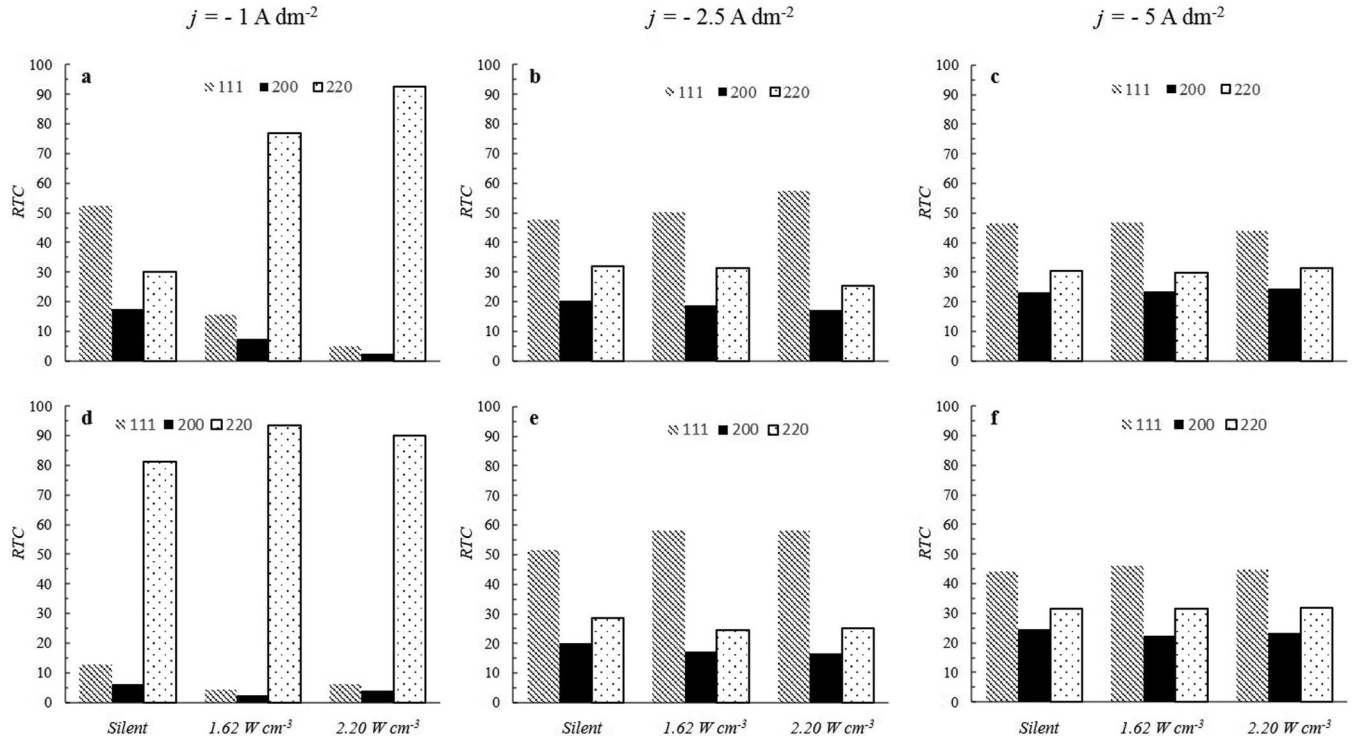

Figure 9. Effect of current density and US irradiation on crystal orientation of deposits obtained (a, b, c) in the absence and (d, e, f) the presence of P-7. In all cases, MNH_2 particles were used.

Addition of P-7 to the plating bath led to a sharp increase in $RTC_{(220)}$ at $j = 1$ A dm^{-2} even for silent conditions (Fig. 9d), but has no meaningful effect on texture for higher current densities. Considering the additives usually adsorb on metal surfaces in a narrow potential range,[83] this behavior is not unexpected. Finally, it is worth mentioning, the same trends were observed when M41 particles were used and thus are not shown in the present work. However, since different particle contents were attained at the same experimental condition for both kinds of particles, it can be concluded that SiO_2 incorporation has virtually no effect on crystal orientation of the deposits.

Conclusions

Cu-SiO_2 composite coatings were prepared using an alkaline non-cyanide electrolyte and synthesized mesoporous M41 particles. Relatively low particle contents were achieved when deposition was carried out in silent conditions at various current densities. However, the incorporation of SiO_2 was significantly enhanced by application of 37 Hz ultrasonic irradiation making it possible to reach silica contents of 5.2 wt%. This beneficial effect of US was only observed at low j, conditions at which the particle-electrode interactions are stronger allowing particles to be embedded in the growing matrix.

Functionalization of M41 particles with aminopropyl groups led to a significant change in the incorporation behavior. First, the amount of codeposited SiO_2 in silent conditions was considerably larger than the one obtained with not functionalized particles. Moreover, in this case US irradiation led to a decrease in the incorporation rate. These differences were ascribed to changes in the surface charging behavior, and probably Cu^{2+} adsorption, induced by the presence of amino groups at the surface of functionalized SiO_2 particles. However, further studies are necessary to fully understand the trends observed in this work. Likewise, the effect of P-7 on particle content depended on the surface chemistry of silica particles.

Besides influencing the codeposition process, US irradiation and P-7 induced variations in the morphology, avoiding cracks formation and promoting nodular growth. However, a synergistic effect between these parameters was observed since smooth surfaces were attained in the presence of P-7 under US irradiation. Finally, it was found that at low current densities both P-7 and US changed the preferred crystal orientation from (111) to (220) but no visible effect at $j > 1$ A dm^{-2} was observed.

Based on these results, it can be concluded that deposition of composite Cu-SiO_2 coating from a Cu**Glu** electrolyte is feasible. Nevertheless, plating parameters (current density, US irradiation, mechanical agitation) as well as particle surface chemistry should be optimized in future investigations. Furthermore, surface functionalization of particles proved to be a great strategy to reach high incorporation rates and should be explore in other metal-particle systems.

Acknowledgments

The authors acknowledge the financial support given by Comisión de Investigaciones Científicas de la Provincia de BuenosAires (CICPBA), Consejo Nacional de Investigaciones Científicas y Técnicas (CONICET) and Universidad Nacional de La Plata (UNLP) for this research. L.N. Bengoa wants to thank UNLP for the funds provided for his research stay in Germany. The authors are also grateful to Dr. Fellenz and Dr. Martin for the synthesis and functionalization of silica particles. Finally, the authors thank Dr. Romanus for the TEM micrographs used in this manuscript.

ORCID

L. N. Bengoa https://orcid.org/0000-0002-0608-8248
A. Ispas https://orcid.org/0000-0001-8203-7752
A. Bund https://orcid.org/0000-0001-9837-2408
W. A. Egli https://orcid.org/0000-0003-0477-660X

References

1. M. J. L. Gines, F. J. Williams, and C. A. Schuh, *J. Appl. Surf. Finish.*, **2**(2), 112 (2007).
2. T. Borkar and S. P. Harimkar, *Surf. Coat. Technol.*, **205**, 4124 (2011).
3. P. Baghery, M. Farzam, A. B. Mousavi, and M. Hosseini, *Surf. Coat. Technol.*, **204**(23), 3804 (2010).
4. L. Benea, P. L. Bonora, A. Borello, and S. Martelli, *Wear*, **249**, 995 (2002).
5. E. García-Lecina, I. García-Urrutia, J. A. Díez, J. Morgiel, and P. Indyka, *Surf. Coat. Technol.*, **206**(11-12), 2998 (2012).
6. S. Alexandridou, C. Kiparissides, J. Fransaer, and J. P. Celis, *Surf. Coat. Technol.*, **71**, 267 (1995).
7. M. Mazaheri M.Ghorbani and A. Afshar, *Surf. Coat. Technol.*, **190**, 32 (2005).
8. I. Tudela, A. J. Cobley, and Y. Zhang, *Friction*, 1 (2018).
9. A. Hovestad, R. J. C. H. L. Heesen, and L. J. J. Janssen, *J. Appl. Electrochem.*, **29**(3), 331 (1999).
10. A. Abdel Aal, H. A. Gobran, and F. Muecklich, *J. Alloys Compd.*, **473**(1-2), 250 (2009).
11. M. Musiani, *Electrochim. Acta*, **45**, 3397 (2000).
12. F. C. Walsh and C. Ponce de Leon, *Trans. Inst. Met. Finish.*, **92**(2), 83 (2014).
13. F. C. Walsh and C. T. J. Low, *Surf. Coat. Technol.*, **304**, 246 (2016).
14. M. D. Gernon, M. Wu, T. Buszta, and P. Janney, *Green Chem.*, **1**(3), 127 (1999).
15. R. Stewart and C. P. Steinecker, Vol. US 2003/0183532 A1, US, 2003.
16. J. C. Ballesteros, E. Chaînet, P. Ozil, G. Trejo, and Y. Meas, *Electrochim. Acta*, **56**(16), 5443 (2011).
17. J. C. Ballesteros, L. M. Torres-Martínez, I. Juárez-Ramírez, G. Trejo, and Y. Meas, *J. Electroanal. Chem.*, **727**, 104 (2014).
18. M. Jung, G. Lee, and J. Choi, *Electrochim. Acta*, **241**, 229 (2017).
19. M. Li, G. Wei, S. Hu, S. Xu, Y. Yang, and Q. Miao, *Surf. Rev. Lett.*, **22**(01), 1550003 (2015).
20. P. S. d. Silva, L. F. d. Senna, and D. C. B. d. Lago, *Mater. Res.*, **20**(suppl 2), 667 (2017).
21. Z. A. Hamid and A. A. Aal, *Surf. Coat. Technol.*, **203**(10–11), 1360 (2009).
22. J. C. Ballesteros, E. Chaînet, P. Ozil, G. Trejo, and Y. Meas, *J. Electroanal. Chem.*, **645**(2), 94 (2010).
23. A. E. Bolzán, *Electrochim. Acta*, **113**, 706 (2013).
24. D. Grujicic and B. Pesic, *Electrochim. Acta*, **50**(22), 4426 (2005).
25. C. G. Fink and J. D. Prince, *Transactions of the American Electrochemical Society*, **54**, 315 (1928).
26. S. Arai, T. Saito, and M. Endo, *J. Electrochem. Soc.*, **157**(3), D147 (2010).
27. J. L. Stojak, J. Fransaer, and J. B. Talbot, in *Advances in Electrochemical Science and Engineering*, R. C. Alkire and D. M. Kolb, eds., Vol. 7, Wiley-VCH, Germany, (2002).
28. A. Bund and D. Thiemig, *J. Appl. Electrochem.*, **37**, 345 (2007).
29. M. K. Camargo, U. Schmidt, R. Grieseler, M. Wilke, and A. Bund, *J. Electrochem. Soc.*, **161**(4), D168 (2014).
30. M. Stroumbouli, P. Gyftou, E. A. Pavlatou, and N. Spyrellis, *Surf. Coat. Technol.*, **195**, 325 (2005).
31. J. R. Roos, J. P. Celis, H. Kelchtermans, M. V. Camp, and C. Buelens, *in* "INTERFINISH 80", 1980.
32. S. Arai, T. Saito, and M. Endo, *J. Electrochem. Soc.*, **157**(3), D127 (2010).
33. S. Fu, X. Chen, P. Liu, W. Liu, P. Liu, K. Zhang, and H. Chen, *J. Mater. Eng. Perform.*, **27**(10), 5511 (2018).
34. M. E. Bahrololoom and R. Sani, *Surf. Coat. Technol.*, **192**, 154 (2005).
35. D. Thiemig, A. Bund, and J. B. Talbot, *Electrochim. Acta*, **54**, 2491 (2008).
36. M. R. Vaezi, S. K. Sadrnezhaad, and L. Nikzad., *Colloids Surf., A*, **315**, 176 (2008).
37. M. Lekka, N. Kouloumbi, M. Gajo, and P. L. Bonora, *Electrochim. Acta*, **50**, 4551 (2005).
38. N. Zhou, S. Wang, and F. C. Walsh, *Electrochim. Acta*, **283**, 568 (2018).
39. M. Sajjadnejad, H. Omidvar, M. Javanbakht, R. Pooladi, and A. Mozafari, *Trans. Inst. Met. Finish.*, **92**(4), 227 (2014).
40. M. Sajjadnejad, A. Mozafari, H. Omidvar, and M. Javanbakht, *Appl. Surf. Sci.*, **300**, 1 (2014).
41. M. Silva-Ichante, Y. Reyes-Vidal, F. J. Bácame-Valenzuela, J. C. Ballesteros, E. Arciga, Ş. Ţălu, A. Méndez-Albores, and G. Trejo, *J. Electroanal. Chem.*, **823**, 328 (2018).
42. A. Afshar, M. Ghorbani, and M. Mazaheri, *Surf. Coat. Technol.*, **187**, 293 (2004).
43. T. Nickchi, M. Ghorbani, A. Alfantazi, and Z. Farhat, *Mater. Des.*, **32**, 3548 (2011).
44. P. Berçot, E. Peña-Muñoz, and J. Pagetti, *Surf. Coat. Technol.*, **157**, 282 (2002).
45. V. Terzieva, J. Fransaer, and J. P. Celis, *J. Electrochem. Soc.*, **147**(1), 198 (2000).
46. X. Wang, J. Li, Y. Zhang, and Y. Wang, *J. Alloys Compd.*, **695**, 2124 (2017).
47. R. Grieseler, M. K. Camargo, M. Hopfeld, U. Schmidt, A. Bund, and P. Schaaf, *Surf. Coat. Technol.*, **321**, 219 (2017).
48. A. Afshar and A. Simchi, *Mater. Sci. Eng., A*, **518**(1-2), 41 (2009).
49. Y. Raghupathy, A. Kamboj, M. Y. Rekha, N. P. Narasimha Rao, and C. Srivastava, *Thin Solid Films*, **636**, 107 (2017).
50. M. Eslami, H. Saghafian, F. Golestani-fard, and A. Robin, *Appl. Surf. Sci.*, **300**, 129 (2014).
51. J. P. Celis, J. R. Roos, C. Buelens, and J. Fransaer, *Trans. Inst. Met. Finish.*, **69**(4), (1991).
52. L. Stappers, Y. Yuan, and J. Fransaer, *J. Electrochem. Soc.*, **152**(7), C457 (2005).
53. M. K. Camargo, I. Tudela, U. Schmidt, A. J. Cobley, and A. Bund, *Electrochim. Acta*, **198**, 287 (2016).
54. N. Guglielmi, *J. Electrochem. Soc.*, **119**(8), 1009 (1972).
55. J. P. Celis, J. R. Roos, and C. Buelens, *J. Electrochem. Soc.*, **134**, (1987).
56. J. Fransaer, J. P. Celis, and J. R. Roos, *J. Electrochem. Soc.*, **139**(2), 413 (1992).
57. A. Hovestad and L. J. J. Janssen, *J. Electrochem. Soc.*, **25**, 519 (1995).

58. A. Hovestad and L. J. J. Janssen, in *Modern Aspects of Electrochemistry No. 38*, B. E. Conway, C. G. Vayenas, R. E. White, and M. E. Gamboa-Adelco, eds., Vol. **38**, Kluwer Academic /Plenum Publishers, New York, (2005).
59. I. Tudela, Y. Zhang, M. Pal, I. Kerr, T. J. Mason, and A. J. Cobley, *Surf. Coat. Technol.*, **264**, 49 (2015).
60. C. Zanella, M. Lekka, and P. L. Bonora, *Surf. Eng.*, **26**(7), 511 (2013).
61. I. Tudela, Y. Zhang, M. Pal, I. Kerr, and A. J. Cobley, *Surf. Coat. Technol.*, **259**, 363 (2014).
62. L. N. Bengoa, P. Pary, and W. A. Egli, *J. Electrochem. Soc.*, **163**(14), D780 (2016).
63. N. Fellenz, P. Martin, S. Marchetti, and F. Bengoa, *J. Porous Mater.*, **22**(3), 729 (2015).
64. M. V. Lombardo, M. Videla, A. Calvo, F. G. Requejo, and G. J. Soler-Illia, *J. Hazard. Mater.*, **223–224**, 53 (2012).
65. R. Saad, K. Belkacemi, and S. Hamoudi, *J. Colloid Interface Sci.*, **311**(2), 375 (2007).
66. P. Pary, L. N. Bengoa, and W. A. Egli, *J. Electrochem. Soc.*, **162**(7), D275 (2015).
67. M. Grün, K. K. Unger, A. Matsumoto, and K. Tsutsumi, *Microporous Mesoporous Mater.*, **27**(2–3), 207 (1999).
68. J. S. Beck, J. C. Vartuli, W. J. Roth, M. E. Leonowicz, C. T. Kresge, K. D. Schmitt, C. T. W. Chu, D. H. Olson, E. W. Sheppard, S. B. McCullen, J. B. Higgins, and J. L. Schlenker, *J. Am. Chem. Soc.*, **114**(27), 10834 (1992).
69. Royal Institue of Technology, Sweden. /www.kth.se/che/medusa
70. L. P. Bérubé and G. L'Espérance, *J. Electrochem. Soc.*, **136**(8), 2314 (1989).
71. I. I. Slowing, J. L. Vivero-Escoto, B. G. Trewyn, and V. S. Y. Lin, *J. Mater. Chem.*, **20**(37), 7924 (2010).
72. N. A. Fellenz, J. F. Bengoa, M. V. Cagnoli, and S. G. Marchetti, *J. Porous Mater.*, **24**(4), 1025 (2017).
73. P. P. Martin, M. F. Agosto, J. F. Bengoa, and N. A. Fellenz, *J. Environ. Chem. Eng.*, **5**(1), 1210 (2017).
74. L. K. Koopal, *Electrochim. Acta*, **41**(14), 2293 (1996).
75. M. Kosmulski, *J. Colloid Interface Sci.*, **337**(2), 439 (2009).
76. S.-F. Cheah, J. Gordon E. Brown, and G. A. Parks, *J. Colloid Interface Sci.*, **208**, 110 (1998).
77. D. Čakara, M. Kobayashi, M. Skarba, and M. Borkovec, *Colloids Surf., A*, **339**(1), 20 (2009).
78. H. Yoshida and N. Kishimoto, *Chem. Eng. Sci.*, **50**(14), 2203 (1995).
79. N. N. Vlasova, *Colloid J.*, **67**(5), 537 (2005).
80. G. Micera, L. S. Erre, and R. Dallocchio, *Colloids Surf.*, **28**(0), 147 (1987).
81. J. P. Fitts, P. Persson, G. E. Brown Jr, and G. A. Parks, *J. Colloid Interface Sci.*, **220**(1), 133 (1999).
82. S. W. Banovic, K. Barmak, and A. R. Marder, *J. Mater. Sci.*, **34**(13), 3203 (1999).
83. M. Paunovic and M. Schlesinger, in *Fundamentals of Electrochemical Deposition*, p. 177, John Wiley & Sons, Inc., (2006).